Metal Complexes (Co^{3+}, Fe^{3+}, Mn^{3+}) of the Quinquedentate Salen Analogue, 2-Methyl-4-benzylthio-*N,N'*-butane-1,2-diylbis(salicylideneimine): Crystal Structures and Sulphur Co-ordination Effects†

Munetoshi Tomita, Naohide Matsumoto,* Hisako Akagi, Hisashi Ōkawa,* and Sigeo Kida
Department of Chemistry, Faculty of Science, Kyushu University, Hakozaki, Higashiku, Fukuoka 812, Japan

Three metal complexes, [Co(L)(Him)]PF_6 (Him = imidazole), [Fe(L)Cl], and [Mn(L)(CH_3OH)]BPh_4, were obtained using a quinquedentate salen analogue with a pendant sulphur capable of axial co-ordination, 2-methyl-4-benzylthio-*N,N'*-butane-1,2-diylbis(salicylideneimine) (H_2L), and their structures and properties were examined with regard to the axial co-ordination of the pendant sulphur. A six-co-ordinate structure with the imidazole and the pendant sulphur at the axial sites was inferred for [Co(L)(Him)]PF_6 from the electronic specta and electrochemical behaviour. The structure of [Fe(L)Cl] was determined by single-crystal *X*-ray crystallography. The configuration around the metal is a distorted square pyramid with the chloride ion at the axial site; the pendant sulphur is not co-ordinated to the metal ion. The co-ordination geometry of [Mn(L)(CH_3OH)]BPh_4 is pseudo-octahedral, with a short Mn–O(methanol) bond [2.246(3) Å] and a long Mn–S bond [2.798(1) Å]. The electronic spectrum in dichloromethane was characterized by an absorption near 27.3 × 10^3 cm^{-1}, which was tentatively assigned to a charge-transfer transition from the co-ordinated sulphur to the manganese(III) ion.

Quinquedentate salen analogues [H_2salen = *N,N'*-ethylenebis(salicylideneimine)] possessing a pendant group of axial co-ordination have been developed in our laboratory,[1] in the hope of observing the axial co-ordination effect upon the structure, properties, and reactivity of their complexes and to mimic some characteristics relevant to metalloenzymes such as natural oxygen carriers,[2,3] coenzyme vitamin B_{12},[4] *etc.* Salen analogues possessing a thioether or thiol in the pendant group are of particular interest in view of the fact that in many metalloproteins the sulphur co-ordination at the apical position gives rise to significant effects upon the spin state or redox potential at the central metal or upon the reactivity towards substrates at the position *trans* to the sulphur donor atom. For cobalt(II) complexes the axial co-ordination of the thioether sulphur resulted in a change of the ground-state electronic configuration, leading to enhanced reactivity towards molecular oxygen.[1b,c] Further, novel μ-oxo-di-iron(III,IV) complexes have been obtained with salen analogues; the very uncommon low-spin state (S = 1) found for the iron(IV) is presumed to be due to the axial co-ordination of the pendant sulphur.[5,6] Single-crystal *X*-ray analysis for the cobalt(III) complex of 2-methyl-4-ethylthio-*N,N'*-butane-1,2-diylbis(salicylideneimine) have revealed the axial co-ordination of the thioether sulphur with a Co–S distance of 2.25 Å.[7] Its reduction potential (Co^{3+}/Co^{2+}) is significantly high compared with complexes having a nitrogen donor at the apical site. Recent electrochemical investigations of cobalt(II) and copper(II) complexes[8] have suggested that axial co-ordination or the detachment of the pendant sulphur takes place on the electrode according to the geometrical requirement of the oxidized or reduced species. In the hope of gaining further information on sulphur co-ordination effects, cobalt(III), iron(III), and manganese(III) complexes of a new quinquedentate salen analogue, 2-methyl-4-benzylthio-*N,N'*-butane-1,2-diylbis(salicylideneimine) (H_2L, see Figure 1), were synthesized and their structures and properties were examined in view of the axial co-ordination of the pendant sulphur. In addition, a single-crystal *X*-ray analysis was carried out on [Fe(L)Cl] and [Mn(L)(CH_3OH)]BPh_4 to verify the existence (or not) of sulphur co-ordination.

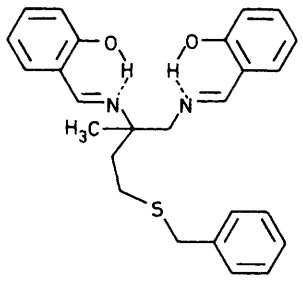

Figure 1. Structure of the ligand H_2L

Experimental

Preparations.—The ligand H_2L was synthesized as yellow prisms (m.p. 83—84 °C) using 4-benzylthio-2-butanone as the starting material *via* the method described previously[1b] (Found: C, 72.05; H, 6.55; N, 6.40. Calc. for $C_{26}H_{28}N_2O_2S$: 72.20; H, 6.55; N, 6.50%).

[Co(L)(Him)]PF_6. A solution of H_2L (0.3 g), imidazole (Him) (0.05 g), and cobalt(II) acetate tetrahydrate (0.17 g) in methanol (20 cm^3) was gently refluxed with stirring for 2 h. Then a methanolic solution of NH_4PF_6 (excess) was added, and the mixture was stirred for 1 h to give a brown precipitate. It was recrystallized from ethanol as brown microcrystals (Found: C, 49.65; H, 4.50; Co, 8.15; N, 6.80. Calc. for $C_{29}H_{30}CoF_6N_4O_2PS$: C, 49.65; H, 4.50; Co, 8.40; N, 7.80%); $\mu_{eff.} \approx 0$; $\Lambda_M(CH_3CN)$ = 126 S cm^2 mol^{-1}.

[Fe(L)Cl]. A mixture of H_2L (0.22 g) and iron(III) chloride (0.08 g) in dry methanol (10 cm^3) was stirred for 1 h to form a purple solution. On evaporating the solvent a purple precipitate was obtained, which was crystallized from chloroform–diethyl ether as dark purple crystals (Found: C, 59.40; H, 5.00; Fe, 11.30; N, 5.35. Calc. for $C_{26}H_{26}ClFeN_2O_2S$: C, 59.85; H, 5.00; Fe, 11.00; N, 5.35%); $\mu_{eff.}$ = 5.95; $\Lambda_M(CH_3CN)$ = 9 S cm^2 mol^{-1}.

[Mn(L)(CH_3OH)]BPh_4. A mixture of H_2L (0.22 g) and

† *Supplementary data available:* see Instructions for Authors, *J. Chem. Soc., Dalton Trans.*, 1989, Issue 1, pp. xvii—xx.

manganese(II) chloride tetrahydrate (0.10 g) in dry methanol (15 cm^3) was stirred for 2 h. To the resulting brown solution was added a methanolic solution of sodium tetraphenylborate (excess), and the mixture was allowed to stand for 2 d to give brown crystals (Found: C, 72.90; H, 6.00; Mn, 6.55; N, 3.35. Calc. for $C_{51}H_{50}BMnN_2O_3S$: C, 73.20; H, 6.00; Mn, 6.55; N, 3.35%); $\mu_{eff.} = 4.95$; $\Lambda_M = 106$ S cm^2 mol^{-1}.

Physical Measurements.—Elemental analyses for C, H, and N were obtained at the Elemental Analysis Service Centre, Kyushu University. Metal analyses were made by atomic absorption spectrometry with a Nippon Jarrel-Ash AA781 atomic absorption and flame emission spectrophotometer. Electrical conductivities were measured on a Denki Kagaku Keiki AOL-10 digital conductometer in acetonitrile; temperature corrections were made. Electronic spectra were recorded on a model MPS-5000 Shimadzu multipurpose spectrophotometer in dichloromethane. Infrared spectra were recorded on a model IR-810 JASCO i.r. spectrometer on KBr discs or Nujol mulls. Magnetic susceptibilities were determined by the Faraday method at room temperature.

Cyclic voltammograms and differential pulse polarograms were measured with a model P-1000 Yanagimoto voltammetric analyser in dichloromethane containing NBu_4ClO_4 (0.1 mol dm^{-3}) as the supporting electrolyte. Measurements were carried out in a three-electrode cell, which was equipped with a glassy carbon working electrode, a platinum coil as the auxiliary electrode, and a calomel electrode as the reference. Potentials were normalized relative to that of the $[Fe(\eta\text{-}C_5H_5)_2]^+$–$[Fe(\eta\text{-}C_5H_5)_2]$ couple[9,10] as internal standard.

X-Ray Structural Determination.—Crystal parameters and details of the data collection and refinements for [Fe(L)Cl] and $[Mn(L)(CH_3OH)]BPh_4$ are given in Table 1. Intensity data were collected on a Rigaku AFC-5 four-circle diffractometer with Mo-K_α radiation monochromated from a graphite crystal at room temperature. Three standard reflections were monitored every 100 reflections and their intensities showed no decay. Intensity data were corrected for Lorentz and polarization effects but not for absorption.

The data were reduced by using the UNICS III programs system[11] of the Computer Center of Kyushu University. The structures were solved by the heavy-atom method and refined by the block-diagonal least-squares method. In the least-squares calculation, equal weights were adopted. Atomic scattering factors were taken from ref. 12. The hydrogen atoms were located by difference-Fourier synthesis and included in the last least-squares calculation. Final difference-Fourier syntheses for both structures are featureless.

Positional parameters of non-hydrogen atoms for [Fe(L)Cl] and $[Mn(L)(CH_3OH)]BPh_4$ are given in Tables 2 and 3, respectively. Additional material available from the Cambridge Crystallographic Data Centre comprises H-atom co-ordinates, thermal parameters, and remaining bond lengths and angles.

Table 1. Summary of crystal data, intensity data collection, and structure refinement

Complex	[Fe(L)Cl]	$[Mn(L)(CH_3OH)]BPh_4$
Formula	$C_{26}H_{26}ClFeN_2O_2S$	$C_{51}H_{50}BMnN_2O_3S$
M	521.78	836.78
Crystal system	Monoclinic	Triclinic
Space group	$P2_1/n$	$P\bar{1}$
a/Å	19.131(9)	13.321(5)
b/Å	8.996(2)	16.592(5)
c/Å	14.098(7)	10.724(4)
α/°	90.0	89.41(2)
β/°	94.57(4)	94.30(5)
γ/°	90.0	113.55(1)
U/Å^3	2 418.9	2 166.3
Z	4	2
D_c/g cm^{-3}	1.394	1.283
D_m/g cm^{-3}	1.39	1.28
Crystal size (mm)	0.4 × 0.3 × 0.4	0.2 × 0.2 × 0.2
μ(Mo-K_α)/cm^{-1}	7.35	3.80
F(000)	1 052	880
Diffractometer	Rigaku AFC-5	Rigaku AFC-5
Scan type	θ–2θ	θ–2θ
Scan width (°)	1.2 + 0.5tanθ	1.2 + 0.5tanθ
Scan rate (°/min^{-1})	6	5
2θ range (°)	2.5—50	2.5—55
Octant measured	$+h$ $+k$, $\pm l$	$+h$, $\pm k$, $\pm l$
No. of unique data	3 292	8 255
No. of parameters	403	717
R	5.26	6.20
R'	4.98	5.87

Results and Discussion

[Co(L)(Him)]PF_6.—The molar conductance determined in acetonitrile is 126 S cm^2 mol^{-1}, which is the expected value for 1:1 electrolyte in this solvent. The electronic spectrum in acetonitrile is given in Figure 2. It shows discernible shoulders around 18 × 10^3 and 21 × 10^3 cm^{-1} attributable to d–d transitions and an intense absorption at 25 × 10^3 cm^{-1}

Table 2. Positional parameters (× 10^4) for [Fe(L)Cl]

Atom	x	y	z	Atom	x	y	z
Fe	1 005(0)	1 715(1)	873(0)	C(11)	433(2)	1 652(4)	−1 462(3)
Cl	1 836(1)	3 500(1)	959(1)	C(12)	262(2)	1 764(5)	−2 448(3)
S	3 836(1)	417(2)	−172(1)	C(13)	−136(2)	2 914(6)	−2 820(3)
O(1)	521(1)	1 948(3)	1 958(2)	C(14)	−379(2)	3 975(5)	−2 223(3)
O(2)	293(1)	2 656(3)	76(2)	C(15)	−231(2)	3 896(5)	−1 260(3)
N(1)	1 548(2)	−61(3)	1 548(2)	C(16)	184(2)	2 729(4)	−858(3)
N(2)	1 097(2)	232(3)	−238(2)	C(17)	2 168(2)	−2 489(5)	1 301(3)
C(1)	666(2)	1 534(4)	2 848(3)	C(18)	2 604(2)	−32(5)	703(3)
C(2)	319(2)	2 198(5)	3 569(3)	C(19)	3 085(2)	−722(5)	23(3)
C(3)	419(2)	1 753(5)	4 494(3)	C(20)	3 435(2)	1 888(6)	−905(4)
C(4)	894(2)	625(5)	4 739(3)	C(21)	3 147(2)	1 401(5)	−1 887(3)
C(5)	1 249(2)	−11(5)	4 064(3)	C(22)	3 557(2)	733(6)	−2 523(4)
C(6)	1 163(2)	417(4)	3 108(3)	C(23)	3 305(3)	351(6)	−3 421(4)
C(7)	1 545(2)	−360(4)	2 428(3)	C(24)	2 618(3)	640(6)	−3 704(3)
C(8)	1 959(2)	−962(4)	898(3)	C(25)	2 206(2)	1 298(7)	−3 093(4)
C(9)	1 459(2)	−1 177(4)	10(3)	C(26)	2 460(2)	1 688(6)	−2 188(4)
C(10)	845(2)	414(4)	−1 101(3)				

Table 3. Positional parameters ($\times 10^4$) for $[Mn(L)(CH_3OH)]BPh_4$

Atom	*x*	*y*	*z*	Atom	*x*	*y*	*z*
Mn	1 337.7(0.4)	1 388.7(0.3)	908.9(0.5)	C(23)	−2 565(4)	1 948(4)	1 851(5)
O_M	1 656(2)	365(2)	−153(3)	C(24)	−2 778(4)	1 929(3)	3 072(4)
C_M	2 250(4)	349(3)	−1 171(5)	C(25)	−1 931(4)	2 358(3)	3 932(4)
S	1 372(1)	2 732(1)	2 491(1)	C(26)	−879(3)	2 791(3)	3 589(4)
O(1)	549(2)	502(1)	1 972(2)	B	5 915(3)	3 253(2)	−2 768(3)
O(2)	53(2)	1 249(1)	−95(2)	C(27)	6 787(2)	3 772(2)	−3 826(3)
N(1)	2 735(2)	1 717(2)	1 964(2)	C(28)	6 454(3)	3 653(2)	−5 094(3)
N(2)	2 259(2)	2 351(2)	−139(2)	C(29)	7 155(3)	4 046(3)	−6 024(3)
C(1)	913(3)	199(2)	2 981(3)	C(30)	8 227(3)	4 594(3)	−5 718(4)
C(2)	162(3)	−549(2)	3 554(3)	C(31)	8 591(3)	4 743(2)	−4 477(4)
C(3)	487(4)	−867(2)	4 621(4)	C(32)	7 879(3)	4 335(2)	−3 550(3)
C(4)	1 545(4)	−474(3)	5 166(4)	C(33)	5 806(3)	2 235(2)	−2 654(3)
C(5)	2 297(4)	245(3)	4 628(4)	C(34)	5 628(4)	1 782(2)	−1 524(4)
C(6)	2 001(3)	592(2)	3 519(3)	C(35)	5 490(4)	910(3)	−1 435(5)
C(7)	2 835(3)	1 342(2)	2 994(3)	C(36)	5 529(4)	453(3)	−2 457(6)
C(8)	3 656(3)	2 545(2)	1 598(3)	C(37)	5 699(4)	864(3)	−3 596(5)
C(9)	3 440(3)	2 629(2)	191(3)	C(38)	5 836(3)	1 738(2)	−3 676(3)
C(10)	1 913(3)	2 729(2)	−1 017(3)	C(39)	4 711(3)	3 242(2)	−3 277(3)
C(11)	782(3)	2 510(2)	−1 424(3)	C(40)	4 600(3)	4 015(2)	−3 657(4)
C(12)	550(3)	3 043(2)	−2 327(3)	C(41)	3 621(4)	4 035(3)	−4 141(4)
C(13)	−507(4)	2 877(3)	−2 764(4)	C(42)	2 692(3)	3 267(3)	−4 273(4)
C(14)	−1 361(3)	2 151(3)	−2 327(4)	C(43)	2 761(3)	2 492(3)	−3 917(4)
C(15)	−1 162(3)	1 606(3)	−1 456(3)	C(44)	3 747(3)	2 483(2)	−3 414(3)
C(16)	−91(3)	1 778(2)	−964(3)	C(45)	6 356(3)	3 779(2)	−1 415(3)
C(17)	4 772(3)	2 482(3)	1 818(3)	C(46)	5 897(3)	4 307(2)	−894(3)
C(18)	3 653(3)	3 315(2)	2 373(3)	C(47)	6 328(4)	4 783(2)	216(3)
C(19)	2 699(3)	3 586(2)	2 166(3)	C(48)	7 327(5)	4 758(2)	837(3)
C(20)	499(4)	3 303(3)	1 980(4)	C(49)	7 727(4)	4 245(3)	381(4)
C(21)	−650(3)	2 811(2)	2 346(3)	C(50)	7 278(4)	3 754(3)	−723(3)
C(22)	−1 510(4)	2 394(4)	1 485(4)				

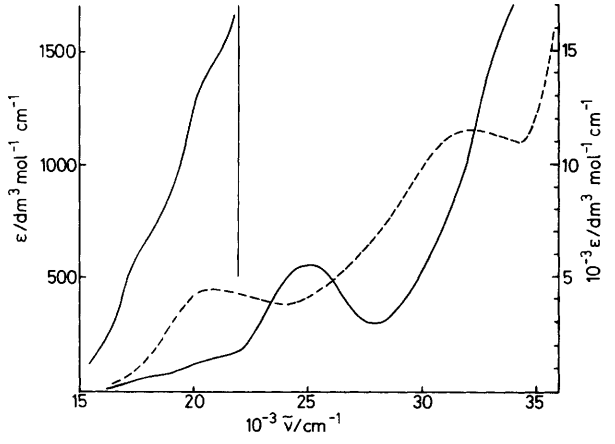

Figure 2. Electronic spectra of (——) $[Co(L)(Him)]PF_6$ in acetonitrile and (— — —) [Fe(L)Cl] in dichloromethane

attributable to a charge-transfer transition. This spectrum bears a marked resemblance to that of $[Co(L')(NH_3)]PF_6$ [H_2L' = 2-methyl-4-ethylthio-*N*,*N*′-butane-1,2-diylbis(salicylideneimine)],[7] whose structure has been determined to be six-co-ordinate with the ammonia and the thioether sulphur at the axial sites. Some five-co-ordinate cobalt(III) complexes of salen and related ligands are known,[13–16] and their electronic spectra are characterized by a well-resolved, intense absorption at a low frequency. Thus, the electronic spectral results indicate that the cobalt is six-co-ordinate with the imidazole and the pendant sulphur at the axial sites.

In the previous study[7] we suggested that the electrochemical technique offers a useful tool to predict the configurations (five-

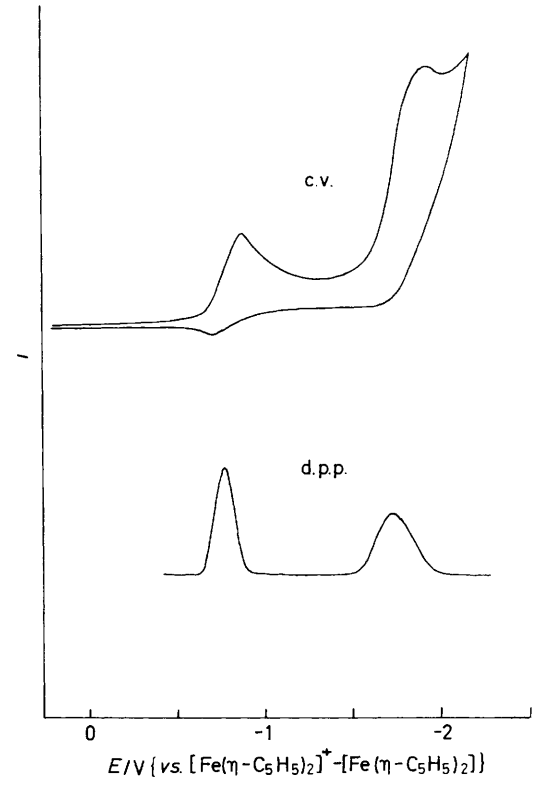

Figure 3. Cyclic voltammogram and differential pulse polarogram of $[Co(L)(Him)]PF_6$ (10^{-4} mol dm^{-3}) in CH_2Cl_2 (0.1 mol dm^{-3} NBu_4ClO_4) at a glassy carbon electrode; scan rate 80 mV s^{-1}

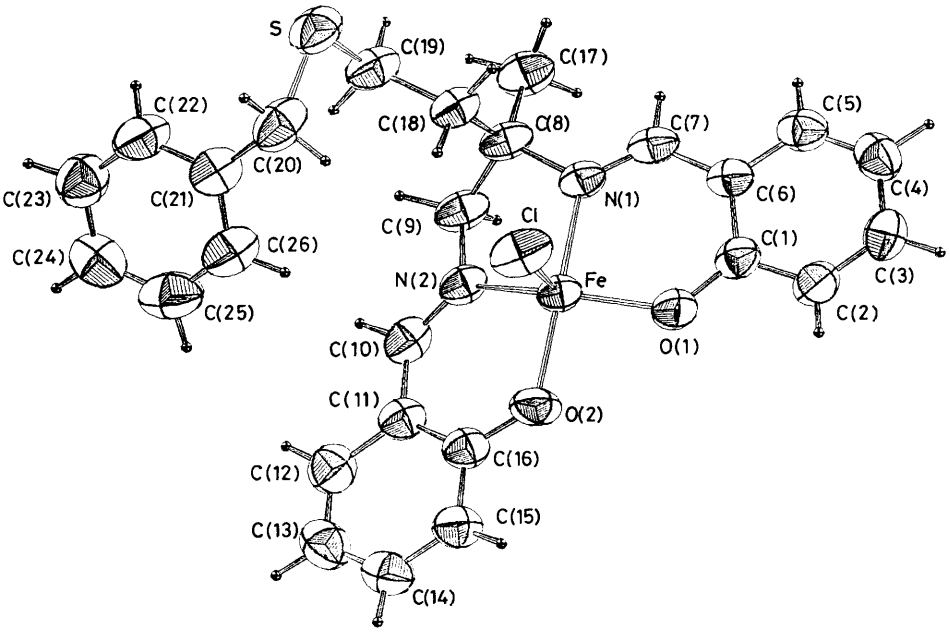

Figure 4. Molecular structure of [Fe(L)Cl] and its numbering scheme

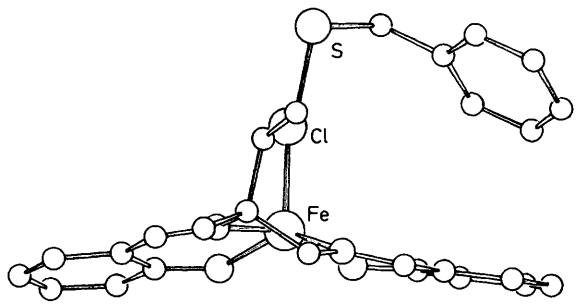

Figure 5. An edge-on view of [Fe(L)Cl]

Table 4. Formal redox potentials (V)[a] of some cobalt(III) complexes

Complex[b]	Co^{III}/Co^{II}	Ref.
$[Co(L')]ClO_4$	−0.36	7
$[Co(L)(Him)]PF_6$	−0.78	This work
$[Co(L')(NH_3)]PF_6$	−0.87	7
$[Co(salen)(CH_3NH_2)_2]PF_6$	−1.03	7
$[Co(salen)(C_2H_5NH_2)_2]PF_6$	−1.06	7

[a] *vs.* $[Fe(\eta\text{-}C_5H_5)_2]^+$–$[Fe(\eta\text{-}C_5H_5)_2]$. [b] L,L′ defined in text.

or six-co-ordination) and the axial donor atoms of cobalt(III) complexes with salen and related ligands. In order to obtain evidence for axial co-ordination of the pendant sulphur, the cyclic voltammogram (c.v.) of $[Co(L)(Him)]PF_6$ was measured in dichloromethane (Figure 3). It showed two reduction waves but no oxidation wave up to +1.0 V. The wave near −0.8 V can be assigned to the Co^{III}/Co^{II} process and the wave at lower potential to the Co^{II}/Co^{I} process.[17] Because of the irreversibility of the waves, the potentials determined by the differential pulse polarogram (d.p.p.) are tentatively taken as formal redox potentials. The Co^{III}/Co^{II} potentials of $[Co(L)(Him)]PF_6$ and related complexes are given in Table 4. For the Co^{II}/Co^{I} process, a detailed discussion is not given here because the potential of this process is practically unaffected by the axial ligands, as established previously.[7] It is seen from Table 4 that the Co^{III}/Co^{II} potential of $[Co(L)(Him)]PF_6$ is comparable to that of $[Co(L')(NH_3)]PF_6$ (six-co-ordination with ammonia and thioether), considerably lower than that of $[Co(L')]ClO_4$ (five-co-ordination with thioether), and significantly higher than those of diaminecobalt(III) complexes, $[Co(salen)(R\text{-}NH_2)_2]PF_6$ (six-co-ordinated with two amines[18]). The results strongly suggest six-co-ordination for $[Co(L)(Him)]BPh_4$, with the imidazole nitrogen and thioether sulphur at the axial sites. It is further suggested from this study that the substitution of imidazole for the axial ammonia causes a positive shift of the Co^{III}/Co^{II} potential.

[Fe(L)Cl].—The crystal structure of [Fe(L)Cl] was determined by single-crystal *X*-ray structure analysis. The ORTEP plot of the perspective view of the molecule is given in Figure 4, together with the numbering system. An edge-on view of the molecule is shown in Figure 5. Relevant bond distances and angles with estimated standard deviations are given in Table 5.

The pendant sulphur is not involved in co-ordination, and the co-ordination geometry around the iron is depicted as a distorted square-pyramid comprising the basal N_2O_2 donor set of the Schiff base and the axial chloride ion. The iron is displaced by 0.53 Å from the N_2O_2 least-squares plane towards the axial ligand. Hence, the Cl–Fe–N(1), Cl–Fe–N(2), Cl–Fe–O(1), and Cl–Fe–O(2) angles all are significantly larger than 90° and the sum of the O(1)–Fe–N(1), N(1)–Fe–N(2), N(2)–Fe–O(2), and O(2)–Fe–O(1) angles is only 344.4°. Further, the basal N_2O_2 set shows a large distortion towards tetrahedral, where the dihedral angle between the planes defined by Fe,N(1),O(1) and Fe,N(2),O(2) is 45°. This is more clearly seen in an edge-on view (Figure 5). For the related complex, chloro[*N*,*N*′-ethylenebis(salicylideneiminato)]iron(III) two geometric isomers, monomeric [Fe(salen)Cl][19] and dimeric $[\{Fe(salen)Cl\}_2]$,[20] are known, and the structure of the present complex may be compared to monomeric [Fe(salen)Cl]. Inspection of the structures of [Fe(L)Cl] and [Fe(salen)Cl] reveals a smaller distortion in the latter. In this complex the displacement of the metal from the basal plane is 0.49 Å and the

Table 5. Relevant bond distances (Å) and angles (°) for [Fe(L)Cl] and $[Mn(L)(CH_3OH)]BPh_4$

[Fe(L)Cl]

(*a*) Bond distances (Å)

Fe–Cl	2.233(1)	Fe–O(1)	1.859(3)
Fe–O(2)	1.880(3)	Fe–N(1)	2.121(3)
Fe–N(2)	2.096(3)	O(1)–C(1)	1.316(5)
C(1)–C(2)	1.391(6)	C(2)–C(3)	1.372(6)
C(3)–C(4)	1.386(7)	C(4)–C(5)	1.343(6)
C(5)–C(6)	1.398(6)	C(6)–C(7)	1.433(6)
N(1)–C(7)	1.271(5)	N(1)–C(8)	1.494(5)
C(8)–C(9)	1.528(6)	N(2)–C(9)	1.473(5)
N(2)–C(10)	1.283(5)	C(10)–C(11)	1.434(6)
C(11)–C(16)	1.401(6)	C(12)–C(13)	1.363(6)
C(13)–C(14)	1.381(7)	C(14)–C(15)	1.367(6)
C(15)–C(16)	1.410(6)	O(2)–C(16)	1.318(5)
C(8)–C(17)	1.523(6)	C(8)–C(17)	1.523(6)
C(8)–C(18)	1.534(6)	C(18)–C(19)	1.515(6)
S–C(19)	1.802(5)	S–C(20)	1.823(5)
C(20)–C(21)	1.513(7)	C(21)–C(22)	1.377(7)
C(22)–C(23)	1.366(7)	C(23)–C(24)	1.368(7)
C(24)–C(25)	1.358(8)	C(25)–C(26)	1.378(8)
C(21)–C(26)	1.370(6)		

(*b*) Angles (°)

O(1)–Fe–N(1)	87.8(1)	O(2)–Fe–N(2)	86.3(1)
O(1)–Fe–O(2)	93.7(1)	N(1)–Fe–N(2)	76.5(1)
Cl–Fe–O(1)	106.6(1)	Cl–Fe–O(2)	101.9(1)
Cl–Fe–N(1)	101.3(1)	Cl–Fe–N(2)	113.4(1)

$[Mn(L)(CH_3OH)]^+$

(*a*) Bond distances (Å)

$Mn–O_M$	2.246(3)	Mn–S	2.798(1)
Mn–O(1)	1.864(2)	Mn–O(2)	1.885(2)
Mn–N(1)	1.982(2)	Mn–N(2)	1.980(2)
O(1)–C(1)	1.328(4)	C(1)–C(2)	1.415(4)
C(2)–C(3)	1.368(5)	C(3)–C(4)	1.379(6)
C(4)–C(5)	1.369(5)	C(5)–C(6)	1.413(5)
C(6)–C(7)	1.440(4)	N(1)–C(7)	1.286(4)
N(1)–C(8)	1.504(3)	C(8)–C(9)	1.531(4)
N(2)–C(9)	1.467(4)	N(2)–C(10)	1.283(4)
C(10)–C(11)	1.434(5)	C(11)–C(12)	1.404(5)
C(11)–C(16)	1.419(4)	C(12)–C(13)	1.368(6)
C(13)–C(14)	1.392(5)	C(14)–C(15)	1.377(6)
C(15)–C(16)	1.399(5)	O(2)–C(16)	1.329(4)
C(8)–C(17)	1.532(5)	C(8)–C(18)	1.532(5)
C(18)–C(19)	1.510(6)	S–C(19)	1.825(3)
S–C(20)	1.823(5)	C(20)–C(21)	1.498(5)
C(21)–C(22)	1.365(5)	C(22)–C(23)	1.387(7)
C(23)–C(24)	1.357(7)	C(24)–C(25)	1.358(5)
C(25)–C(26)	1.371(5)	C(21)–C(26)	1.387(5)

(*b*) Angles (°)

O(1)–Mn–O(2)	91.9(1)	O(1)–Mn–N(1)	93.4(1)
O(2)–Mn–N(2)	91.7(1)	N(1)–Mn–N(2)	82.8(1)
O_M–Mn–O(1)	87.7(1)	O_M–Mn–O(2)	94.3(1)
O_M–Mn–N(1)	92.0(1)	O_M–Mn–N(2)	92.6(1)
C_M–O_M–Mn	136.5(2)	O_M–Mn–S	167.9(1)
S–Mn–O(1)	93.3(1)	S–Mn–O(2)	97.6(1)
S–Mn–N(1)	75.9(1)	S–Mn–N(2)	85.5(1)

dihedral angle between the planes defined by Fe,N(1),O(1) and Fe,N(2),O(2) is 41.2°.

The ethylene chain of the salen skeleton adopts a *gauche* conformation, with the benzylthioethyl residue in the axial and the methyl group in the equatorial position. The equatorially oriented methyl group is expected to exert a steric effect towards the neighbouring azomethine proton,[21] and this steric interaction must be the main reason for the larger distortion (towards tetrahedral) in this complex. Another noticeable feature is that the fifth ligand (chloride) and the benzylthioethyl residue are posed on the same side.

Iron(III) complexes of salen and related Schiff bases often adopt a dimeric structure, bridged through the phenolic oxygen in out-of-plane mode,[20] and show a sub normal magnetic moment.[20,22,23] However, the single-crystal *X*-ray analysis reveals that this is not the case for [Fe(L)Cl]. In accord with its monomeric structure, a powdered sample of [Fe(L)Cl] shows a magnetic moment of 5.95 at room temperature which is very close to the spin-only value expected for high-spin iron(III). The electronic spectrum of [Fe(L)Cl] determined in dichloromethane (Figure 2) resembles that of [Fe(salen)Cl][24] and shows absorption bands at 20.8×10^3 and 32.2×10^3 cm^{-1}.

$[Mn(L)(CH_3OH)]BPh_4$.—The presence of co-ordinated methanol was evidenced by the observation of the O–H stretching mode at 3 170 cm^{-1}. Unlike [Mn(salen)Cl] and related complexes[25] which exhibit a sub normal magnetic moment at room temperature, the magnetic moment of $[Mn(L)(CH_3OH)]BPh_4$ (4.95 at room temperature) is common for high-spin manganese(III).

The perspective drawing of the complex cation is shown in Figure 6, where the numbering scheme adopted is exactly the same as that in [Fe(L)Cl]. An edge-on view of the cation is given in Figure 7. The structure of the tetraphenylborate anion is not given because the anion is far apart from the cation and does not seem to affect its structure. Selected bond lengths and angles are given in Table 5.

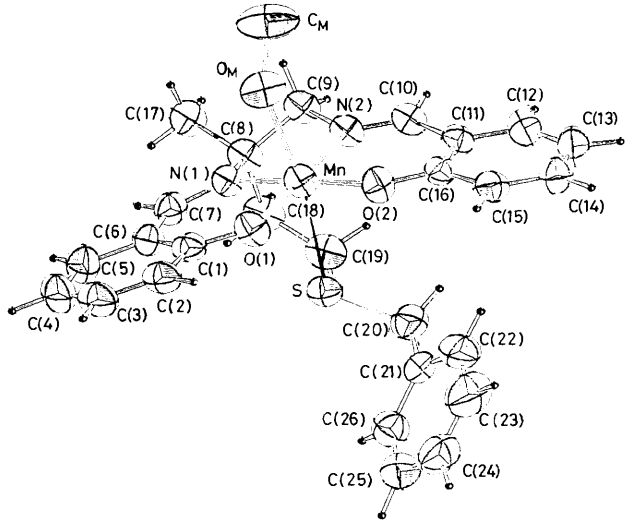

Figure 6. Structure of $[Mn(L)(CH_3OH)]^+$ and its numbering scheme

The configuration around the metal is elongated octahedral with the pendant sulphur and a methanol molecule at the axial sites, showing a Jahn–Teller distortion due to the high-spin d^4 configuration. Strong co-ordination of the methanol to the metal is inferred from the Mn–O(methanol) bond distance (2.246(3) Å). On the other hand, the Mn–S bond is significantly long (2.798(1) Å). This fact suggests that the manganese(III) ion prefers an oxygen donor to a sulphur donor. The in-plane

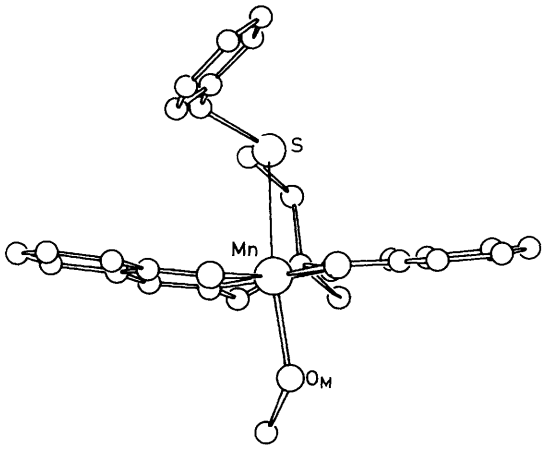

Figure 7. An edge-on view of $[Mn(L)(CH_3OH)]^+$

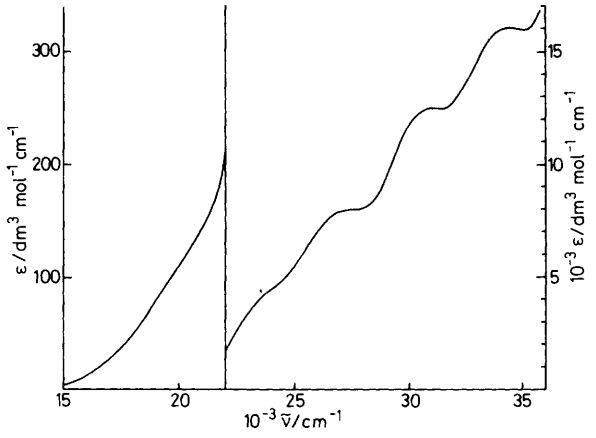

Figure 8. Electronic spectrum of $[Mn(L)(CH_3OH)]BPh_4$ in dichloromethane

Mn–O and Mn–N distances are comparable to those of $[\{Mn(salen)(Him)\}_2][ClO_4]_2$ and $[Mn(salen)(dimb)][ClO_4]_2$ [dimb = 1,4-di(1-imidazolyl)butane][26] and also to those of [Mn(acen)Cl] [H_2acen = *N*,*N*′-ethylenebis(acetylacetoneimine)].[27] The Mn–O distances are comparable to the Fe–O distances of [Fe(L)Cl], whereas the Mn–N distances are considerably shorter than the Fe–N distances of [Fe(L)Cl]. The basal MnN_2O_2 part shows only a small tetrahedral distortion (Figure 7) where the dihedral angle is 6.1°. The metal is displaced by 0.05 Å from the basal mean plane (N_2O_2) towards the apical methanol oxygen. The Mn–O(methanol) bond is nearly perpendicular to the mean plane whereas the Mn–S bond deviates considerably from perpendicularity towards N(1). Thus the N(1)–Mn–S angle is only 75.9° and thence the O(methanol)–Mn–S angle (167.9°) is significantly smaller than 180° {*cf.* the H_3N–Co–S angle of $[Co(L')(NH_3)]PF_6$ (178.1°), which is very close to 180°}.[7] The large distortion in the present complexes is undoubtedly ascribed to the long Mn–S bonding. The ethylene chain of the salen skeleton also adopts a *gauche* conformation, with the pendant group in the axial position so as to allow sulphur co-ordination to the metal.

The electronic spectrum of the manganese complex in dichloromethane is shown in Figure 8, which exhibits five absorptions in the region 15×10^3—35×10^3 cm^{-1}. All the absorptions (except that at 27.3×10^3 cm^{-1}) are commonly seen for manganese(III) complexes of salen and related ligands[25,28] for spectra measured in non-polar solvents like chloroform. The absorption at 20×10^3 cm^{-1} is assigned to a *d*–*d* band,[29] two absorptions at 23.5×10^3 and 31.0×10^3 cm^{-1} to charge-transfer bands,[30] and the absorption at 34.5×10^3 cm^{-1} to an intra-ligand band.[30] Therefore, the electronic spectrum of $[Mn(L)(CH_3OH)]BPh_4$ is characterized by a new absorption at 27.3×10^3 cm^{-1}. In view of the *X*-ray structural result which demonstrates the axial co-ordination of the pendant sulphur to the metal, we believe that the sulphur co-ordination is maintained in solution and the band at 27.3×10^3 cm^{-1} can be assigned to a charge-transfer transition from the sulphur to Mn^{III}.

References

1 (*a*) W. Kanda, H. Ōkawa, and S. Kida, *Bull. Chem. Soc. Jpn.*, 1983, **56**, 3268; (*b*) K. Nakamoto, H. Oshio, H. Ōkawa, W. Kanda, K. Horiuchi, and S. Kida, *Inorg. Chim. Acta*, 1985, **108**, 231; (*c*) W. Kanda, H. Ōkawa, S. Kida, J. Goral, and K. Nakamoto, *ibid.*, 1988, **146**, 193.
2 M. F. Perutz, *Nature (London)*, 1970, **228**, 726.
3 J. C. Kendrew, *Science*, 1963, **139**, 1259.
4 C. Brink-Shoemaker, D. W. J. Cruickshank, D. C. Hodgkin, M. J. Kamper, and D. Pilling, *Proc. R. Soc. London, Ser. A*, 1964, **278**, 1.
5 H. Ōkawa, K. Horiuchi, W. Kanda, H. Oshio, and S. Kida, *Bull. Chem. Soc. Jpn.*, 1986, **59**, 2795.
6 K. Horiuchi, M. Koikawa, S. Baba, H. Ōkawa, Y. Maeda, H. Oshio, and S. Kida, *Inorg. Chim. Acta*, 1988, **144**, 99.
7 K. Horiuchi, M. Mikuryia, H. Ōkawa, and S. Kida, *Bull. Chem. Soc. Jpn.*, 1987, **60**, 3575.
8 Presented at the Annual Meeting of Chemical Society of Japan, Fukuoka, 1987.
9 R. R. Gagne, C. A. Koval, and G. C. Lisensky, *Inorg. Chem.*, 1980, **19**, 2854.
10 H. M. Koepp, H. Wendt, and H. Strehlow, *Z. Electrochem.*, 1975, **64**, 483.
11 T. Sakurai and K. Kobayashi, *Rikagaku Kenkyusho Houkoku*, 1979, **55**, 69; S. Kawano, *Rep. Comput. Cent, Kyushu Univ.*, 1980, **13**, 39.
12 'International Tables for *X*-Ray Crystallography,' Kynoch Press, Birmingham, 1975, vol. 4.
13 M. Calvin, R. H. Bailes, and W. K. Wilmarth, *J. Am. Chem. Soc.*, 1946, **68**, 2254; M. Calvin and C. H. Barkelew, *ibid.*, p. 2267; R. H. Bailes and M. Calvin, *ibid.*, 1947, **69**, 1886.
14 G. Costa, G. Mestroni, and L. Stefani, *J. Organomet. Chem.*, 1967, **7**, 493.
15 Y. Aimoto, W. Kanda, S. Meguro, Y. Miyahara, H. Ōkawa, and S. Kida, *Bull. Chem. Soc. Jpn.*, 1985, **58**, 646.
16 C. W. Smith, G. W. Van Loon, and M. C. Baird, *Can. J. Chem.*, 1976, **54**, 1875.
17 D. F. Averill and R. F. Broman, *Inorg. Chem.*, 1978, **17**, 3389.
18 S. Maeda, M. Nakamura, M. Mikuriya, T. Shinmyozu, H. Ōkawa, and S. Kida, *Mem. Fac. Sci. Kyushu Univ., Ser. C*, 1985, **15(1)**, 63.
19 M. Gerloch and F. E. Mabbs, *J. Chem. Soc. A*, 1967, 1598.
20 M. Gerloch and F. E. Mabbs, *J. Chem. Soc. A*, 1967, 1900.
21 A. Pasini, M. Gullotti, and R. Ugo, *J. Chem. Soc., Dalton Trans.*, 1977, 346; R. S. Downing and F. L. Urbach, *J. Am. Chem. Soc.*, 1969, **91**, 5977; M. Calligaris, G. Nardin, and L. Randaccio, *J. Chem. Soc., Dalton Trans.*, 1973, 419; D. Hall, T. N. Waters, and P. E. Wright, *ibid.*, p. 1508.
22 M. Gerloch, J. Lewis, F. E. Mabbs, and A. Richards, *J. Chem. Soc. A*, 1968, 112.
23 W. M. Rieff, G. J. Long, and W. A. Baker, jun., *J. Am. Chem. Soc.*, 1968, **90**, 6347.
24 T. Tsumaki, *Bull. Chem. Soc. Jpn.*, 1938, **13**, 583.
25 L. J. Boucher and M. O. Farrell, *J. Inorg. Nucl. Chem.*, 1973, **35**, 3731.
26 N. Matsumoto, N. Takemoto, A. Ohyoshi, and H. Ōkawa, *Bull. Chem. Soc. Jpn.*, 1988, **61**, 2984.
27 L. J. Boucher and V. W. Day, *Inorg. Chem.*, 1977, **16**, 1360.
28 L. J. Boucher and C. G. Coe, *Inorg. Chem.*, 1976, **15**, 1334.
29 L. J. Boucher and D. R. Herrington, *Inorg. Chem.*, 1974, **13**, 1105.
30 R. S. Downing and F. L. Urbach, *J. Am. Chem. Soc.*, 1969, **91**, 5977; *ibid.*, 1970, **92**, 5861.

Received 13*th April* 1988; *Paper* 8/01440J